

## Characterization of the Porous Boron $\delta$ -Doped Si Superlattice

T. C. Chang, M. Y. Hsu, C. Y. Chang, C. P. Lee, T. G. Jung, W. C. Tsai,  
G. W. Hunag, and Y. J. Mei  
Institute of Electronics, National Chiao Tung University  
Hsinchu, Taiwan, R.O.C.

In this work, we report the first study of the porous boron  $\delta$ -doped Si superlattice. Visible photoluminescence (PL) with multiple peaks from the porous boron  $\delta$ -doped Si superlattice was observed at room temperature. The multiple peaks of PL spectrum from the porous superlattice can be explained on the basis of interference from the periodic structure.

### 1. INTRODUCTION

It is now well established that porous silicon, prepared by the electrochemical etching of crystalline wafers in hydrofluoric acid, readily emits visible light at room temperature when illuminated by high energy photons.<sup>1,2)</sup> It has been observed that Si quantum wire networks are found during electrochemical and chemical dissolution of bulk wafers.<sup>3)</sup> The emission of light has been attributed to quantum size effects resulting from the remnant Si skeleton in the porous layer of sufficiently small dimensions.<sup>1,3)</sup> The expected dependence of the luminescence peak position on porosity has been observed.<sup>4)</sup> Quantum size effects have also been invoked to explain visible photoluminescence in Si microcrystalline powder,<sup>5)</sup> and in nonocrystals of indirect bandgap semiconductor, such as Ge and AgBr.<sup>6,7)</sup> An alternative explanation, chemical rather than physical, is that visible luminescence from porous silicon was originated from the hydride ( $\text{SiH}_x$ ), or in Si-O-H compounds derived from siloxene ( $\text{Si}_6\text{O}_3\text{H}_6$ ),<sup>8,9)</sup> Another group of researches emphasized the importance of the amorphization of the silicon layer in producing luminescent material. Nevertheless, the origin of visible luminescence from porous silicon remains to be clarified.

Most of researches about porous Si were the conventional porous Si which were directly prepared by the electrochemical etching of crystalline wafers. In this work, we report the first study of the porous boron  $\delta$ -doped Si superlattice. Visible photolumines-

cence (PL) with multiple peaks from the porous boron  $\delta$ -doped Si superlattice was observed at room temperature. The multiple peaks of PL spectrum from the porous superlattice can be explained on the basis of interference from the periodic structure.

### 2. EXPERIMENTAL

The epitaxial boron  $\delta$ -doped Si superlattice was grown on 10  $\Omega$  cm, p-type, (001) Si substrates using a home-made hot-wall multiwafer ultrahigh vacuum/chemical vapor deposition (UHV/CVD) system. The growth temperature was kept constant at 550  $^\circ\text{C}$ . Silane ( $\text{SiH}_4$ ) was used as reactant gases. In addition, 1% diborane ( $\text{B}_2\text{H}_6$ ) in hydrogen was used as the p-type dopant gas. The base pressure of the system was maintained at about  $2 \times 10^{-8}$  Torr in the growth chamber. During growth, the system was operated at about 1.0 mTorr.

The porous boron  $\delta$ -doped Si superlattice was formed by anodizing an as-grown boron  $\delta$ -doped Si superlattice in a HF-ethanol solution (HF:  $\text{C}_2\text{H}_5\text{OH}$ :  $\text{H}_2\text{O} = 1:1:2$ ) at a current density of 12.5  $\text{mA}/\text{cm}^2$  for 3 min. A platinum wire was used for the cathode of the electrolytic cell. Before anodization, the as-grown superlattice was cleaned, and an ohmic contact was formed by evaporating thin Al film onto the back surface to ensure a uniform anodic current distribution.

### 3. RESULTS AND DISCUSSION

In the figure 1, curve (a) shows HRXRD rocking curve for the as-grown boron  $\delta$ -doped Si superlattice grown on (001) Si substrate. This superlattice consisted of 51 periods of boron  $\delta$ -doped Si. In this figure, peak Sub represents the Si substrate reflection, peak P0 the zeroth-order superlattice reflection, and other main peaks are nth-order satellite peaks (-2, -1, +1, +2), resulting from the periodicity of the superlattice. Curve (b) represents the simulated rocking curve for a Si/Si-B superlattice of 51 periods with Si layer 28 nm thick, Si-B layer 3.1 nm thick with boron concentration of  $1.75 \times 10^{20} \text{ cm}^{-3}$ . When compared to curve (a), good matches between experiment and simulation in terms of peak position and peak intensity of each main peak are clearly observed. Therefore, boron  $\delta$ -doped Si superlattice with high crystalline quality could be achieved by UHV/CVD. Moreover, such a boron concentration in the Si-B layers exceeds the solid solubility of boron at the growth temperature by more than two order of magnitude. The highly none-equilibrium property of the Si-B epilayer grown by the UHV/CVD technique had been reported previous.<sup>10,11)</sup>

Fig. 2 shows the room temperature PL spectrum of the porous boron  $\delta$ -doped Si superlattice. Visible photoluminescence with multiple peaks were observed from this periodic structure. This result is very different from that of conventional porous Si structures which were directly etched the Si substrate. In our work, only one broaden peak was observed in conventional porous Si at the same etching condition. In contrast, there are six peaks were observed in the porous boron  $\delta$ -doped Si superlattice. The multiple peaks of PL spectrum from the porous boron  $\delta$ -doped Si superlattice can be explained on the basis of interference from the periodic structure.

To confirm our postulate, Fig. 3 shows a typical cross-sectional SEM micrograph of this porous boron  $\delta$ -doped Si superlattice. The sample was cleaved and examined directly by SEM without further modification. The periodic and layered structure of the porous boron  $\delta$ -doped Si superlattice was clearly observed. The thickness of period was measured to be  $31 \pm 2 \text{ nm}$ . This value agrees with that of the as-grown boron  $\delta$ -doped Si superlattice.

Fig. 4 shows the theoretical transmittance curve for multilayer dielectric film of 51 periods with high index of refraction ( $n=3$ ) layer 28 nm thick and low index of refraction ( $n=2.8$ ) layer 3.1 nm thick. This transmittance curve is caused by the interference from this multilayer. The high and low index of refraction represent the porous Si and the porous Si-B regions,

respectively. The refractive index of porous Si can be estimated to be the combination of crystalline silicon and air (void) with the Bruggeman effective medium approximation.<sup>12)</sup> Since the porosity of high doping region is higher than that of undoped region at the same etching condition, the index of refraction of porous Si is higher than that of porous Si-B regions. In this figure, six peaks occurred in the transmittance curve. This result agree with the observation of six peaks in the PL experiment. Therefore, the multiple peaks of PL for porous boron  $\delta$ -doped Si superlattice was due to the interference of this periodic structure with alternative refractive index.

### 4. CONCLUSION

We report the first study on the porous boron  $\delta$ -doped Si superlattice. Visible photoluminescence (PL) with multiple peaks from the porous boron  $\delta$ -doped Si superlattice was observed at room temperature. The multiple peaks of PL spectrum from the porous superlattice can be explained on the basis of interference from the periodic structure.

#### Acknowledgment

This work was performed at National Nano Device Laboratory which was supported in part by the National Science Council of Republic of China under contract No. NSC 82-0404-E009-233.

### 5. REFERENCES

- 1) L. T Canham, *Appl. Phys. Lett.* **57** (1990) 1046.
- 2) N. Koshiada and H. Koyaman, *Jpn. J. Appl. Phys.* **30** (1991) L1221.
- 3) A. G. Cullis and L. T. Canham, *Nature* **353** (1991) 335.
- 4) A. Bsiesy, J. C. Vial, F. Gaspard, R. Herino, M. Ligeon, F. Muller, R. Romestain, A. Wasiela, A. Halimaoui, and G. Bomchil, *Surf. Sci.* **254** (1991) 195.
- 5) H. Takagi, H. Ogawa, A. Yamazaki, and T. Nakagiri, *Appl. Phys. Lett.* **59** (1991) 3168.
- 6) Y. Meada, N. Ysukamoto, Y. Kancemitsu, and Y. Masumoto, *Appl. Phys. Lett.* **59** (1990) 3168.
- 7) K. P. Johansson, G. Mclendon, and P. A. Marchetti, *Chem. Phys. Lett.* **179** (1991) 321.
- 8) C. Tsai, K. H. Li, J. Sarathy, S. Shin, J. C. Campbell, B. Hance, and J. M. White, *Appl. Phys. Lett.* **59** (1991) 2814.

- 9) M. S. Brandt, H. D. Stutzmann, J. Weber, M. Cardona, *Solid State Commun.* **81** (1992) 307.
- 10) B. S. Meyerson, F. K. LeGoues, T. N. Nguyen and D. L. Harnam, *Appl. Phys. Lett.* **50** (1987) 113.
- 11) T. C. Chang, C. Y. Chang, T. G. Jung, W. C. Tasi, G. W. Huang and P. J. Wang, *Jpn. J. Appl. Phys. Part 1*, **33** (1994) 309.
- 12) C. Pickering, M. I. J. Beale, D. J. Robbins, P. J. Pearson and R. Greef, *Thin Solid Film* (1984) 157.

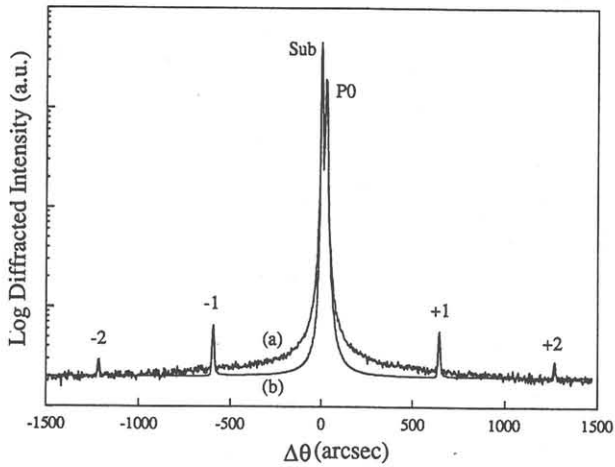


FIG. 1 (a) HRXRD rocking curve for boron  $\delta$ -doped Si superlattice grown on (001) Si substrate; (b) simulated rocking curve for a Si/Si-B superlattice of 51 periods with Si layer 28 nm thick, Si-B layer 3.1 nm thick with boron concentration of  $1.75 \times 10^{20} \text{ cm}^{-3}$ .

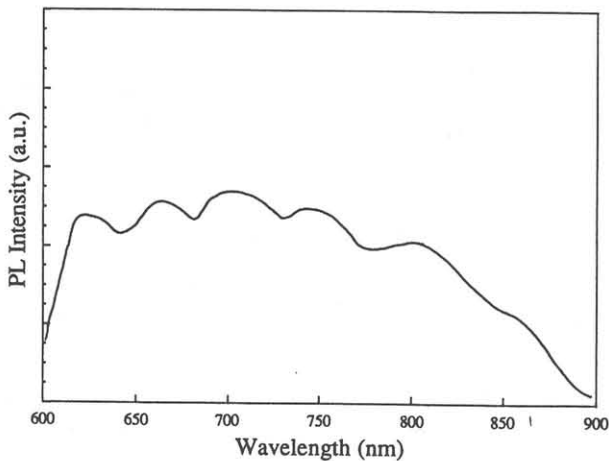


FIG. 2 Room temperature photoluminescence spectrum of the porous boron  $\delta$ -doped Si superlattice. Multiple peaks were observed in this spectrum.

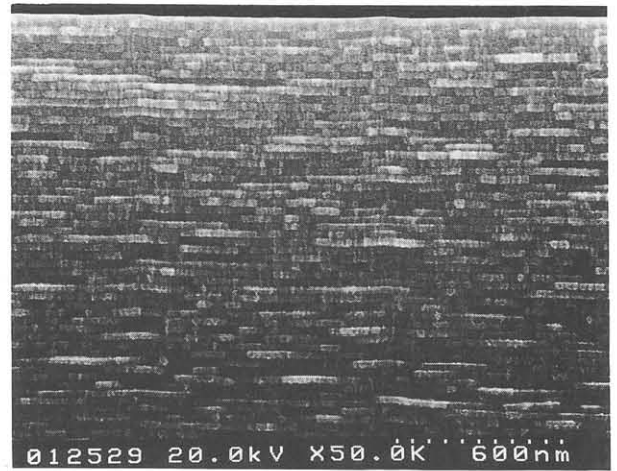


FIG. 3 Cross-section SEM micrograph of the porous boron  $\delta$ -doped Si superlattice

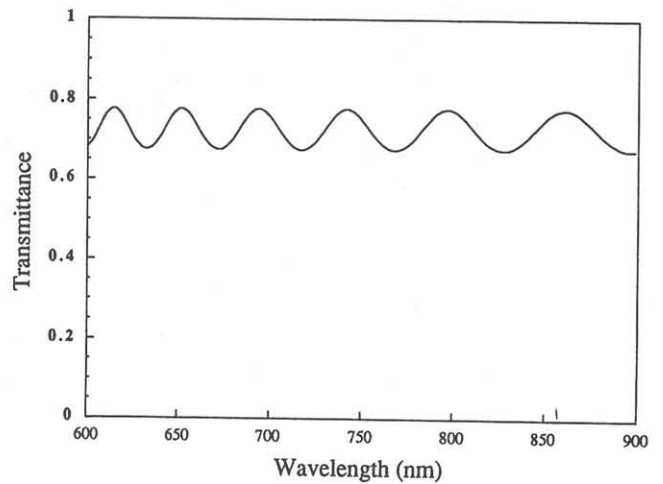


FIG. 4 Theoretical transmittance curve for multilayer dielectric film of 51 periods with high index of refraction ( $n=3$ ) layer 28 nm thick and low index of refraction ( $n=2.8$ ) layer 3.1 nm thick.